

Supplementary materials for

## Influence of luminescent properties of powders on fabrication of scintillation ceramics by stereolithography 3D printing

L.V. Ermakova, V.V. Dubov, R.R. Saifutyarov, D.E. Kuznetsova, M.S. Malozovskaya,  
P.V. Karpyuk, G.A. Dosovitskiy, P.S. Sokolov

*Institute of Chemical Reagents and High Purity Chemical Substances of NRC "Kurchatov  
institute" (IREA), 107076 Moscow, Bogorodskiy val 3, Russia*

This PDF file includes:

Characterization of as-synthesized garnet powders and as-prepared UV-cured slurries.

Figures S1, S2, S3, S4.

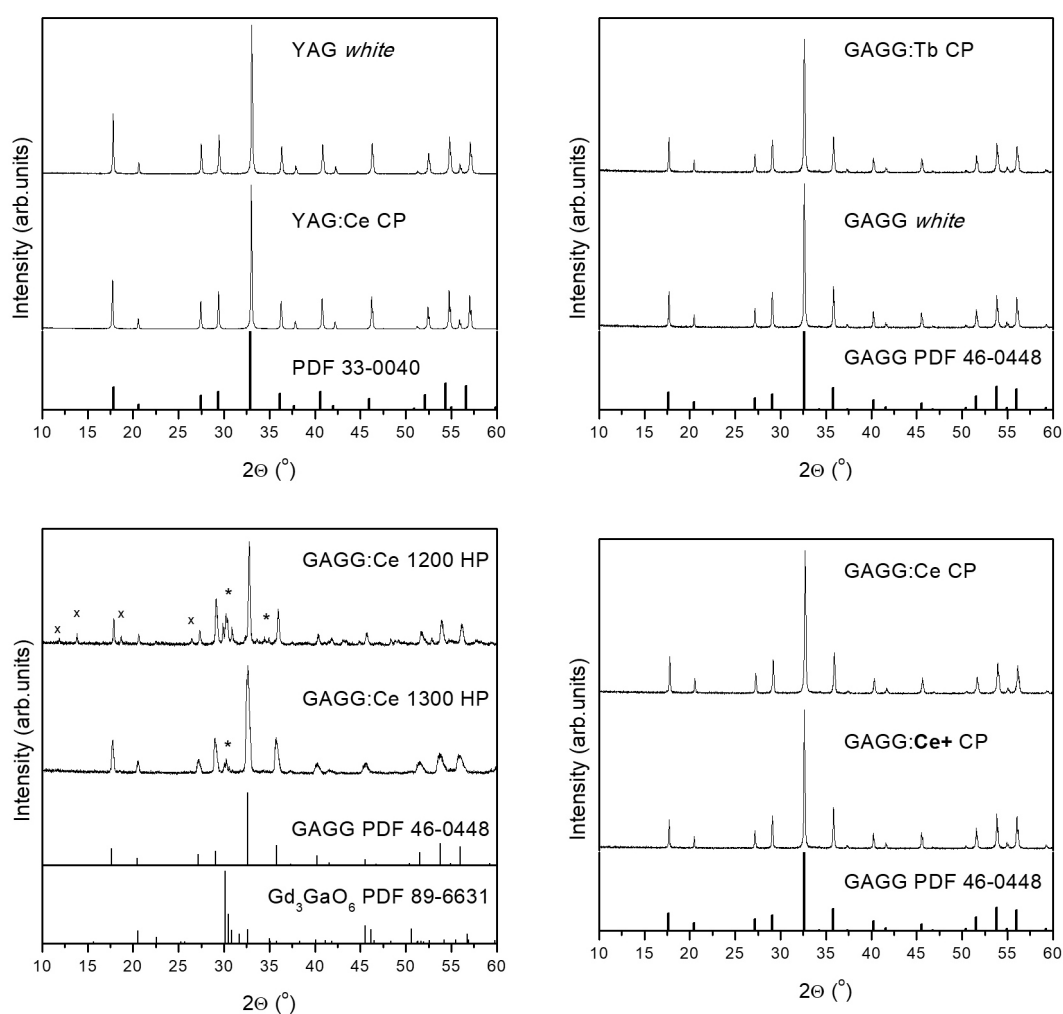


**Fig. S1.** XRD patterns of the powders used in the work. Lines for the  $Y_3Al_5O_{12}$  garnet phase are given at the bottom of each graph after PDF # 33-0040, and for the  $Gd_3Al_2Ga_3O_{12}$  garnet phase after PDF # 46-0448. The stars \* shows the location of diffraction lines of  $Gd_3GaO_6$  (PDF # 89-6631) and x other impurity phase(s).

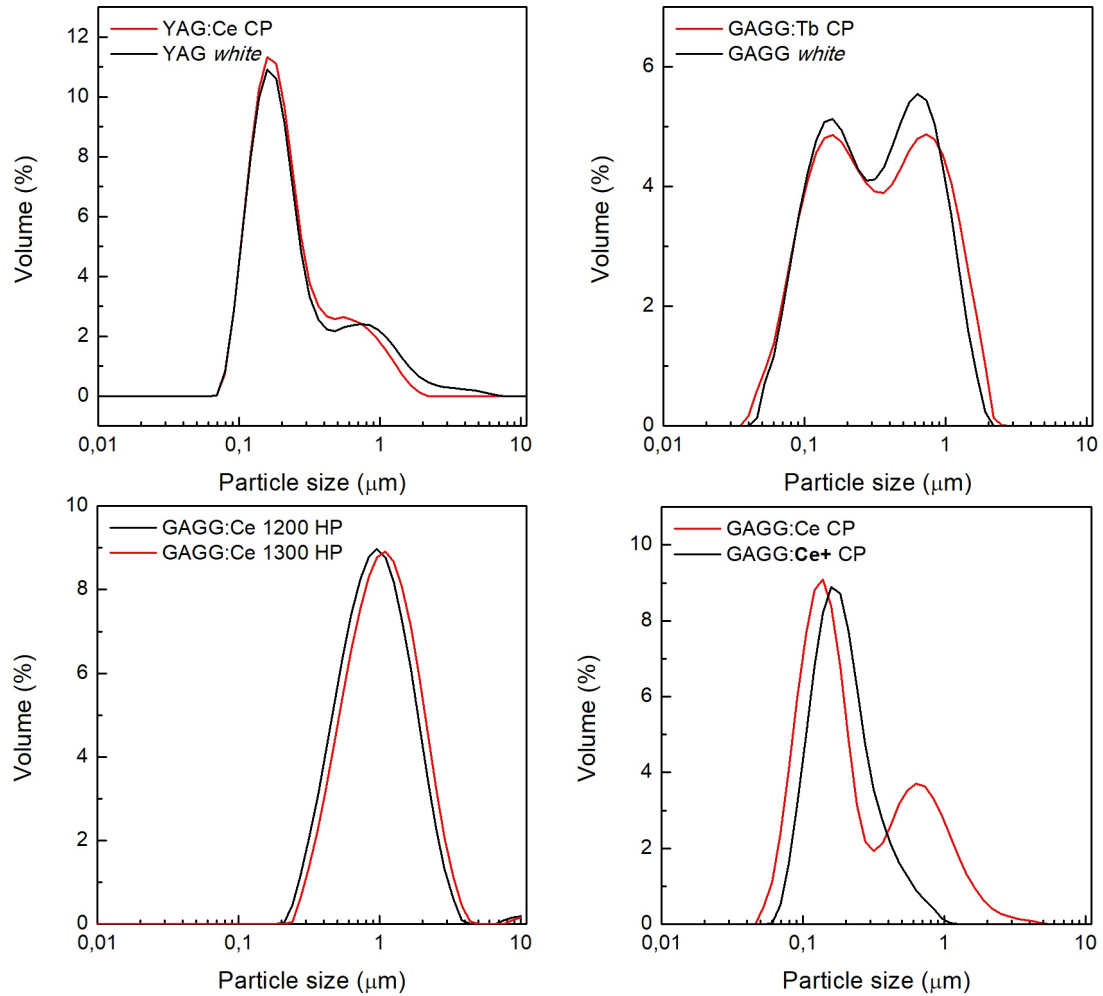
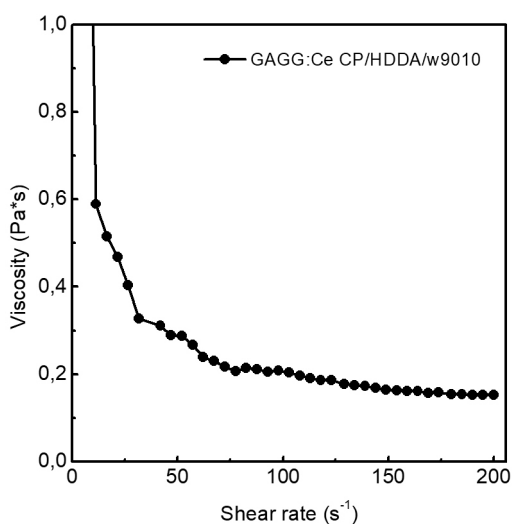
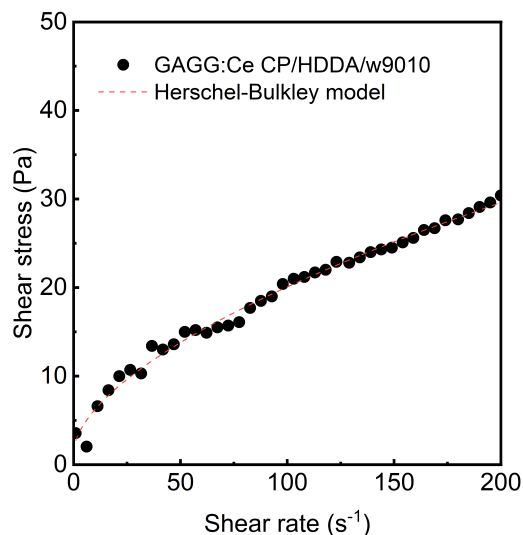


**Fig. S2.** Particle size distributions of the powders used in the work.

All the suspensions for measuring particle size distribution (PSD) in this work were prepared and analyzed in the same way according to ISO13320:2009. No dispersant or surfactant was used during measurement. The small portion of the suspension (~0.5 ml) was taken immediately after milling and stirred up with 10 ml of water in a laboratory ultrasonic bath. Then this diluted suspension was directly transferred into the instrument. Distilled water was used as the liquid phase in the Hydro G dispersing attachment; the attachment pumped the measured powder suspension diluted in distilled water through the measurement cuvette, which was set in Mastersizer 2000 apparatus, with simultaneous stirring and ultrasonic agitation, ensuring that the powder was suspended and not settled down. PSD was calculated from the raw data with the Mastersizer software (Ver. 5.60) based on Mie scattering theory. Refractive indexes of 1.85 and 1.90 were used for YAG and GAGG powders respectively. An absorption index of 0.1 was used in both cases.

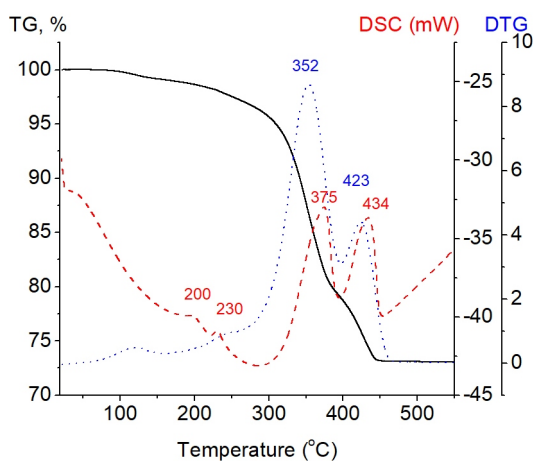


(a)

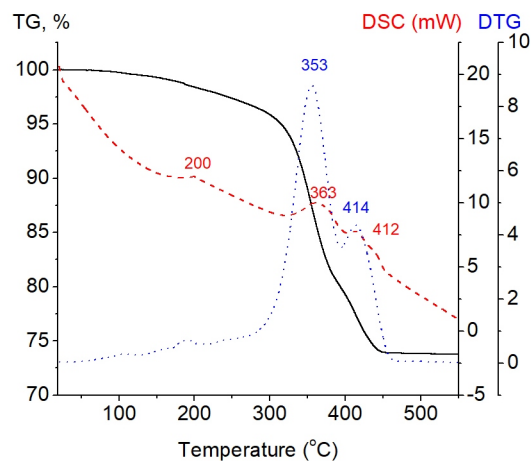


(b)

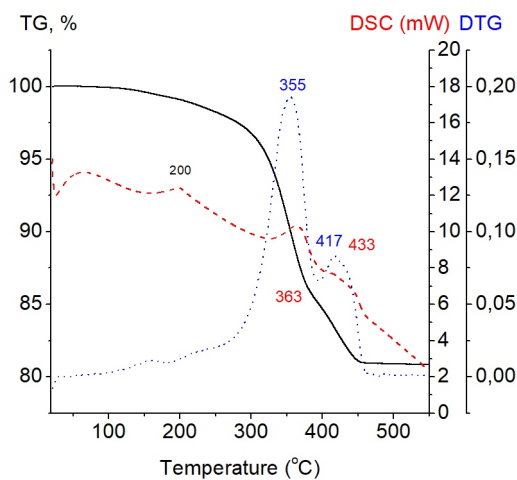
**Fig. S3.** Viscosity (a) and shear stress (b) *versus* shear rate for the slurry of GAGG:Ce CP HDDA/w9010/TPO-L at 20.0 °C. The gray dash-line represent the Herschel-Bulkley model fitted with parameters  $\tau_0=1.6(8)$ ,  $K=1.18(25)$ ,  $n=0.599(036)$ ,  $R^2 = 0.99$ .



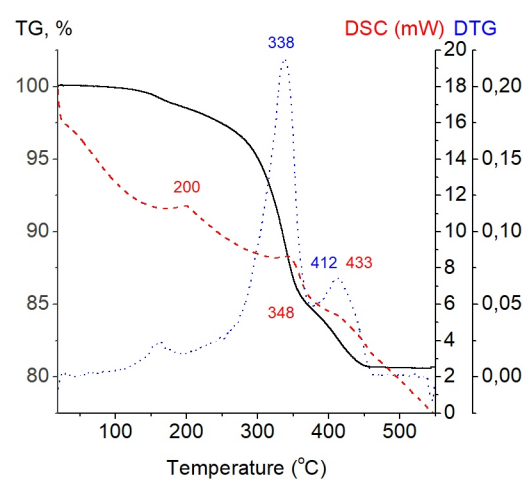
(a)



(b)



(c)



(d)

**Fig. S4.** TG (black solid lines), DTG (blue dotted lines) and DSC (red dashed lines) curves of the cured composites with HDDA/w9010/TPO-L for YAG *white* (a), YAG:Ce CP (b), GAGG:Tb CP (c) and GAGG:Ce CP (d) when heated in flow air at rate 2.5 K/min.

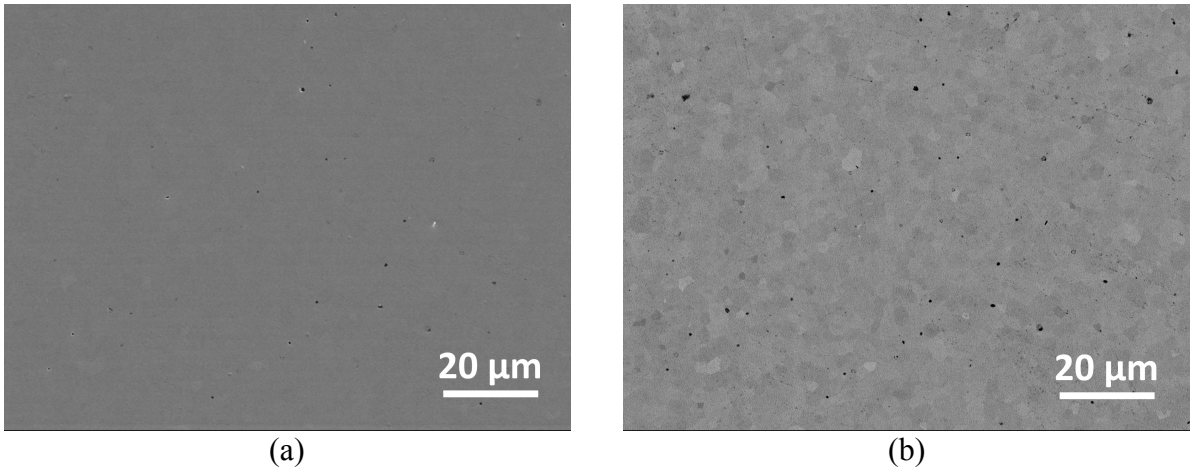


**Fig. S5.** SEM images of a cross-section of the 3D printed ceramic sample from GAGG:Ce HP 1300 powder, (a) secondary electrons mode, (b) backscattered electrons mode. No thermal etching was performed, the contrast settings were set to maximum in BSE mode to reveal separate grains by orientation contrast.

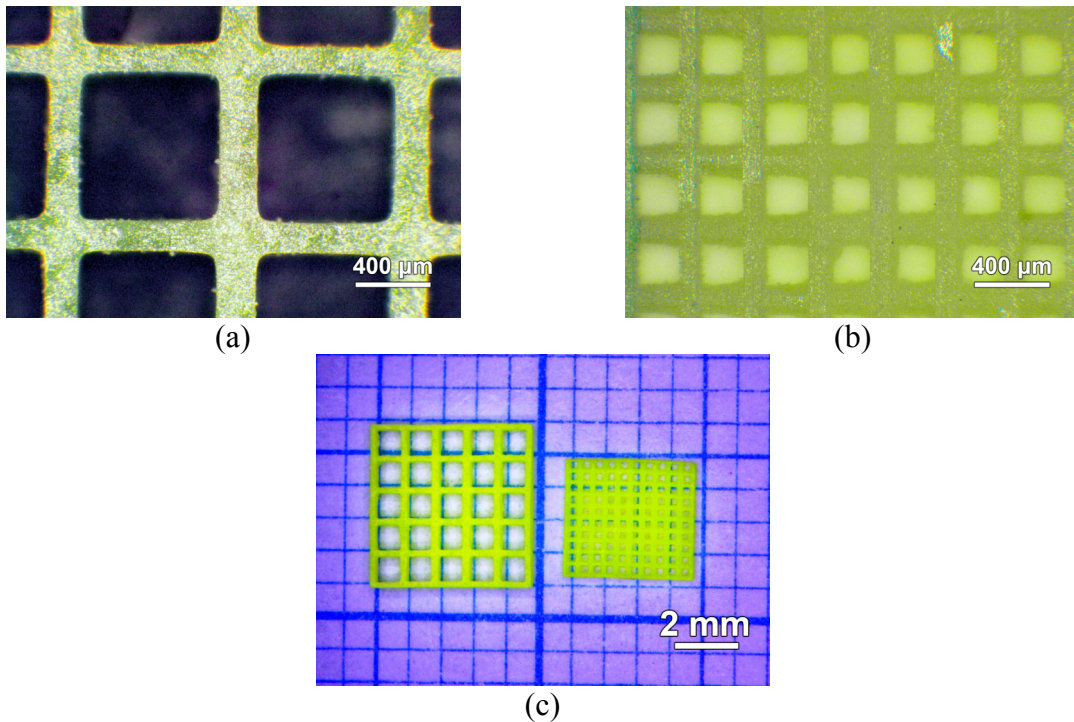


**Fig. S6.** Optical microscopy images of sintered ceramics of additional printed geometries – orthogonal meshes with different cell sizes (a, b), and photograph of these ceramic samples (c).